RNA (2001), *7*:671–681. Cambridge University Press. Printed in the USA.

Mutation in the *prp12*$^+$ gene encoding a homolog of SAP130/SF3b130 causes differential inhibition of pre-mRNA splicing and arrest of cell-cycle progression in *Schizosaccharomyces pombe*

YASUAKI HABARA,[1,3] SEIICHI URUSHIYAMA,[1,4] TOSHIHARU SHIBUYA,[1] YASUMI OHSHIMA,[1] and TOKIO TANI[1,2]

[1]Department of Biology, Graduate School of Sciences, Kyushu University, Hakozaki, Higashi-ku, Fukuoka 812-8581, Japan
[2]PRESTO, Japan Science and Technology Corporation, Hakozaki, Higashi-ku, Fukuoka 812-8581, Japan

ABSTRACT

***prp12-1* is one of the mutants defective in pre-mRNA splicing at a nonpermissive temperature in *Schizosaccharomyces pombe.* We found that the *prp12*$^+$ gene encodes a protein highly homologous with a human splicing factor, SAP130/SF3b130, a subunit of a U2 snRNP-associated complex SF3b. Prp12p was shown to interact genetically with Prp10p that is a homolog of SAP155/SF3b155, another subunit in SF3b, suggesting that Prp12p is a functional homolog of human SAP130/SF3b130. Prp12p tagged with GFP is uniformly localized in the nuclear DNA region. In addition to pre-mRNA splicing defects, the *prp12-1* mutant produced elongated cells, a typical phenotype of cell division cycle (*cdc*) mutants, suggesting a possible link between pre-mRNA splicing and cell-cycle progression. We examined kinetics of splicing defects in *prp12-1* and several other *prp* mutants using northern blot hybridization and found that, among all the tested pre-mRNAs, only *TfIId*$^+$ pre-mRNA with low splicing efficiency showed detectable splicing defects at the nonpermissive temperature in *prp12-1*. In addition, we found that other *prp* mutants with the *cdc* phenotype also showed differential splicing defects in tested pre-mRNAs at the nonpermissive temperature. On the other hand, *prp* mutants that do not exhibit the *cdc* phenotype showed a rapid and complete block of pre-mRNA splicing in all the tested pre-mRNAs at the nonpermissive temperature, indicating that *prp* mutants with weak splicing defects have a tendency to exhibit the *cdc* phenotype. These results suggest that the *cdc* phenotype in *prp12-1* is caused by a selective reduction of spliced transcripts encoding a protein (or proteins) required for G2/M transition.**

Keywords: *cdc*; fission yeast; intron; mutant; *prp*; SF3b; spliceosome associated protein

INTRODUCTION

The accurate removal of an intron from a nuclear pre-mRNA, a process known as pre-mRNA splicing, is essential for gene expression in eukaryotic cells. Pre-mRNA splicing takes place within a large complex termed a spliceosome, which contains small nuclear ribonucleoprotein particles (U1, U2, U4/U6, and U5 snRNPs) and a large number of non-snRNP proteins. A series of non-snRNP proteins essential for pre-mRNA splicing was identified biochemically using a mammalian in vitro splicing system and genetically using budding yeast *Saccharomyces cerevisiae.* To identify novel factors involved in pre-mRNA splicing, we and others have isolated *prp* (pre-mRNA processing) mutants of fission yeast *Schizosaccharomyces pombe*, which are defective in pre-mRNA splicing at the nonpermissive temperature.

So far, 14 *prp* mutants (*prp1–prp14*) have been isolated in *S. pombe* (Potashkin & Frendewey, 1989; Rosenberg et al., 1991; Urushiyama et al., 1996; Potashkin et al., 1998). At the nonpermissive temperature, these mutants are defective in pre-mRNA splicing and accumulate pre-mRNAs in cells. Interestingly, cell bodies in 8 of 14 *prp* mutants are elongated at the nonpermissive temperature, a typical phenotype observed in cell

Reprint requests to: Tokio Tani, Department of Biology, Graduate School of Sciences, Kyushu University, Hakozaki, Higashi-ku, Fukuoka 812-8581, Japan; e-mail: ttaniscb@mbox.nc.kyushu-u.ac.jp.
[3]Present address: Howard Hughes Medical Institute (HHMI), Department of Genetics, Duke University Medical Center, Durham, North Carolina 27710, USA.
[4]Present address: Department of Molecular Cell Biology, Medical Research Institute, Tokyo Medical and Dental University, Kanda-Surugadai, Chiyoda 101-0062, Japan.

division cycle (*cdc*) mutants (Urushiyama et al., 1996; Potashkin et al., 1998). Expression of the *cdc*-like phenotype at the nonpermissive temperature in these mutants indicates a possible relation between pre-mRNA splicing and cell-cycle progression.

The *prp1*$^+$ gene was found to encode a protein with a TPR-motif (Urushiyama et al., 1997) and to be allelic with *zer1* (zero1), which was independently identified as a G0 arrest mutation (K. Okazaki & H. Okayama, unpubl. results). The *prp2*$^+$ gene encodes spU2AF^{59}, a fission yeast homolog of the human U2AF large subunit U2AF^{65} (Potashkin et al., 1993; Wentz-Hunter & Potashkin, 1996). The *prp4*$^+$ gene product is predicted to be a serine/threonine kinase (Alahari et al., 1993; Groß et al., 1997). The *prp10*$^+$ gene encodes a fission yeast homolog of SAP155/SF3b155, a subunit of the splicing factor complex SF3 associated with U2 snRNP (Habara et al., 1998). Mutants of these four genes do not exhibit the *cdc*-like phenotype at the nonpermissive temperature. On the other hand, two of the genes responsible for *prp* mutations with the *cdc* phenotype (*prp5* and *prp8*) were cloned. The *prp5*$^+$ gene encodes a WD repeat protein (McDonald et al., 1999). Physical and genetic interactions between Prp5p and Cdc5p were also reported (McDonald et al., 1999). The *prp8*$^+$ gene, the mutant of which exhibits the typical *cdc* phenotype, was found to be identical with the *cdc28*$^+$ gene encoding a DEAH-box RNA helicase (Lundgren et al., 1996). However, exact mechanisms whereby defects in pre-mRNA splicing cause cell-cycle blocks in these mutants are still unknown.

SF3 is a U2 snRNP-associated multisubunit complex required for binding of U2 snRNA to the branch site. It consists of two subcomplexes, SF3a and SF3b (reviewed in Krämer, 1996; Burge et al., 1999). SF3a and SF3b contain three (SAP61/SF3a60, SAP62/SF3a66, and SAP114/SF3a120) and four subunits (SAP49/SF3b50, SAP130/SF3b130, SAP145/SF3b145, and SAP155/SF3b155), respectively (Krämer et al., 1994; Bennett & Reed, 1993; Krämer, 1995). Using UV crosslinking and a yeast two-hybrid assay, SAP155/SF3b155 was shown to bind to pre-mRNA on both sides of a branch site in the spliceosome complex A and to interact directly with U2AF^{65} (Gozani et al., 1998). It was also noted that SAP155/SF3b155 is associated with cyclin E and is efficiently phosphorylated in vitro by cyclin E-cdk2, a critical regulator of cell-cycle progression from G1 to S phase, suggesting a possible link between pre-mRNA splicing and cell-cycle progression in mammalian cells (Seghezzi et al., 1998).

Here, we report the cloning and characterization of the *S. pombe prp12*$^+$ gene, the mutant of which exhibits the *cdc*-like phenotype at the nonpermissive temperature. The *prp12*$^+$ gene was found to encode a homolog of a SF3b subunit, SAP130/SF3b130. Examination of kinetics of the splicing defects in *prp12-1* and several other *prp* mutants revealed that sensitivities to the *prp* mutations in pre-mRNA splicing are different among tested pre-mRNAs and that *prp* mutants with weak splicing defects show a tendency to exhibit a *cdc*-like phenotype at the nonpermissive temperature.

RESULTS

Cloning of the *prp12*$^+$ gene

To clone the *prp12*$^+$ gene, we transformed the *prp12-1* mutant (SU102-11D) with the *S. pombe* genomic library constructed in cosmid pSS10 (Nakaseko et al., 1986). We isolated cosmids from five independent *ts4*$^+$ transformants. These cosmids were reintroduced into the SU102-11D strain, and we found rescue activity in three of five isolated cosmids. Restriction patterns of these three cosmids shared DNA fragments of the same length, suggesting that these cosmids had an overlapping region. The insert of cosmid #58 was subcloned into pSP1, which is the *S. pombe ars1* multicopy vector (Cottarel et al., 1993). In the course of subcloning, we found that cosmid #58 has a region overlapping with the cosmids used in the fission yeast genome project (Fig. 1A). Because the PstI-3 fragment shown in Figure 1A has rescue activity for temperature sensitivity of *prp12-1*, we sequenced a gapped region between two cosmids, c27E2 and c19G12. This 7.6-kb genomic sequence was registered in the DNA Data Bank of Japan database with the accession number AB034966. After several steps of subcloning, we identified an *Nde*I fragment of 5.7 kb that complements the temperature-sensitive growth of *prp12-1.* Complementation of the splicing defect in *prp12-1* with the *Nde*I 5.7-kb fragment was also verified by northern blot analysis (Fig. 1B, lanes 8 and 9). The fragment was found to contain one ORF encoding a 1,206 amino acid protein (Fig. 1A).

To identify a mutation site in *prp12-1*, we amplified the corresponding ORF from *prp12-1* by PCR and sequenced it. There was a single point mutation at the nucleotide position 3340, resulting in replacement of glycine with serine at the amino acid position 1114 (Fig. 2). Unexpectedly, the temperature sensitivity of *prp12-1* was suppressed with the multicopy introduction of the *prp12-1* mutant gene (data not shown).

To confirm further that the isolated gene is the authentic *prp12*$^+$ gene and not a suppressor gene, we performed integration mapping as described in Materials and Methods. Twenty-three asci were dissected and all the progenies showed cosegregation of *prp12*$^+$ and *ura4*$^+$ in genetic crosses, indicating that the isolated gene is not a suppressor gene (data not shown).

The *prp12*$^+$ gene encodes an SF3b subunit, SAP130

A search of the database using the identified ORF sequence revealed the presence of a Prp12p homolog in

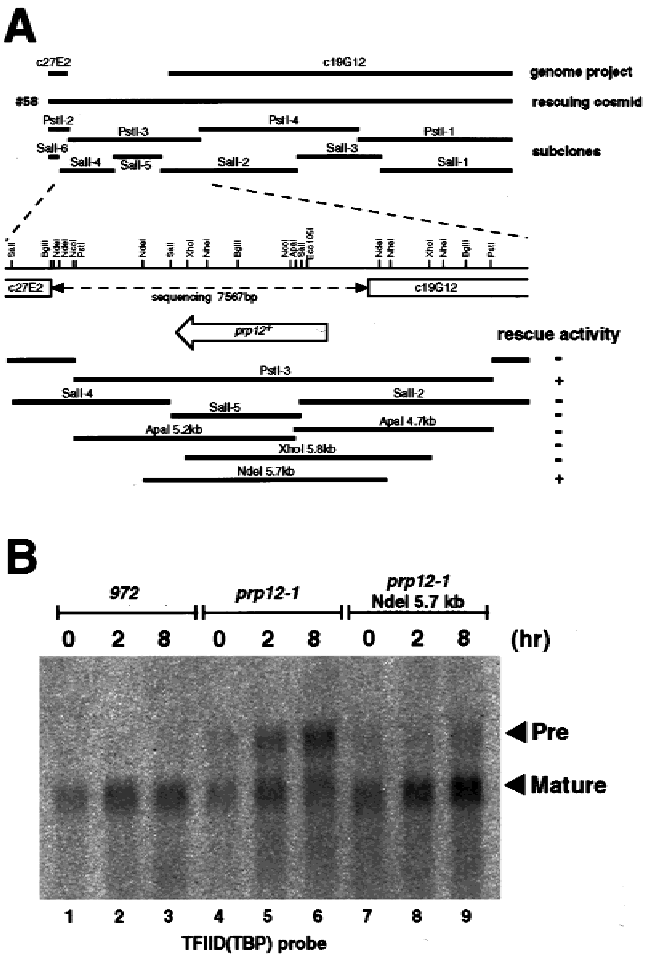

FIGURE 1. A: Location of the *prp12⁺* gene. Ten restriction fragments were isolated from cosmid #58 and subcloned in pSP1 (*Pst*I-1–4 and *Sal*I-1–6). All subclones were introduced into the SU102-11D strain and only *Pst*I-3 showed rescue activity for the temperature sensitivity of *prp12-1.* PstI-3 was then divided into four fragments (*Apa*I 5.2 kb, *Apa*I 4.7 kb, *Xho*I 5.8 kb, and *Nde*I 5.7 kb) and these subclones were tested for complementation. Only the *Nde*I 5.7-kb fragment complemented *prp12-1.* Because the rescue activity was located in the sequence gap between cosmids c27E2 and c19G12, the gapped region was sequenced using *Pst*I-3 and *Sal*I-4 as templates. **B:** Defect in pre-mRNA splicing in the *prp12-1* mutant and complementation of the defect by the isolated genomic fragment. Total RNA was isolated from *972* (a wild-type strain), *prp12-1*, or *prp12-1* transformed with the *Nde*I 5.7-kb fragment, which was grown in an MMA medium at 26 °C and shifted to 37 °C for the time indicated above each lane. Ten micrograms of total RNA were fractionated on a 1% formaldehyde agarose gel and blotted onto a membrane. The membrane was then probed with the TFIID probe.

Caenorhabditis elegans and *S. cerevisiae* (GenPept accession numbers AAB97566 and Q04693, respectively). The gene for the *S. cerevisiae* homolog of Prp12p is *RSE1*, the mutant of which was originally isolated as a temperature-sensitive mutant defective in ER-to-Golgi transport (Chen et al., 1998). Identification of the human U2 snRNP-associated protein, SAP130/SF3b130, was recently reported (Das et al., 1999), and we found that this is the human homolog of Prp12p. Comparison of the amino acid sequence of Prp12p with those of its putative homologs is shown in Figure 2. Overall homologies in amino acid sequence between Prp12p and SAP130/SF3b130 and between Prp12p and RSE1 are 44.4% and 26.5%, respectively. We could not find any known conserved sequence motifs that suggested its function in Prp12p.

Genetic interaction between *prp10* and *prp12*

The fission yeast *prp10⁺* gene encodes a homolog of human SAP155/SF3b155, a subunit of the splicing factor SF3b (Habara et al., 1998). Because the *S. pombe prp12⁺* gene encodes a protein homologous with the human SAP130/SF3b130, another subunit of SF3b, we generated a double mutant carrying *prp12-1* and *prp10-1* mutations and examined their synthetic effects. As a negative control, we used a double mutant with *prp1-4* and *prp12-1*, which shows no synthetic effect on the temperature sensitivity (Urushiyama et al., 1997). As shown in Figure 3, *prp1-4, prp10-1,* and *prp12-1* single mutants and the *prp1-4 prp12-1* double mutant could proliferate normally at 20 °C and 26 °C, but the *prp10-1 prp12-1* double mutant hardly grew at 26 °C and grew very slowly at 20 °C. Such synthetic effects between *prp10-1* and *prp12-1* on temperature sensitivity suggests that Prp12p interacts with Prp10p, supporting the notion that Prp12p is a functional homolog of human SAP130/SF3b130.

Prp12p-GFP is localized in the nucleus

To examine the subcellular localization of Prp12p, we constructed a Prp12p-GFP fusion gene and introduced it into wild-type cells or the *prp12-1* mutant. The fusion gene complemented the temperature-sensitive phenotype of the *prp12-1* mutant, suggesting that the GFP-tagged Prp12p is functional in *S. pombe* (data not shown). As shown in Figure 4, Prp12p-GFP is localized predominantly in the DNA region in the nucleus, which means that Prp12p is a nuclear protein. Nuclear localization of Prp12p-GFP supports further the notion that the *prp12⁺* gene encodes a splicing factor.

The *prp 12-1* mutation causes cell-cycle arrest at the nonpermissive temperature

At the nonpermissive temperature, *prp12-1* produced elongated cells, the typical phenotype of *cdc* mutants (Urushiyama et al., 1996). To further characterize the phenotype, we examined *prp12-1* cytologically by staining with Hoechst 33342. Wild type, *prp12-1,* and *cdc10-129* were grown at 26 °C in minimum media and then shifted to 37 °C. *cdc10-129* was used as a control for the *cdc* phenotype. Cells were collected and stained at 0, 2, 4, 6, and 8 h after the shift to the nonpermissive temperature. After 4 h at the nonpermissive tempera-

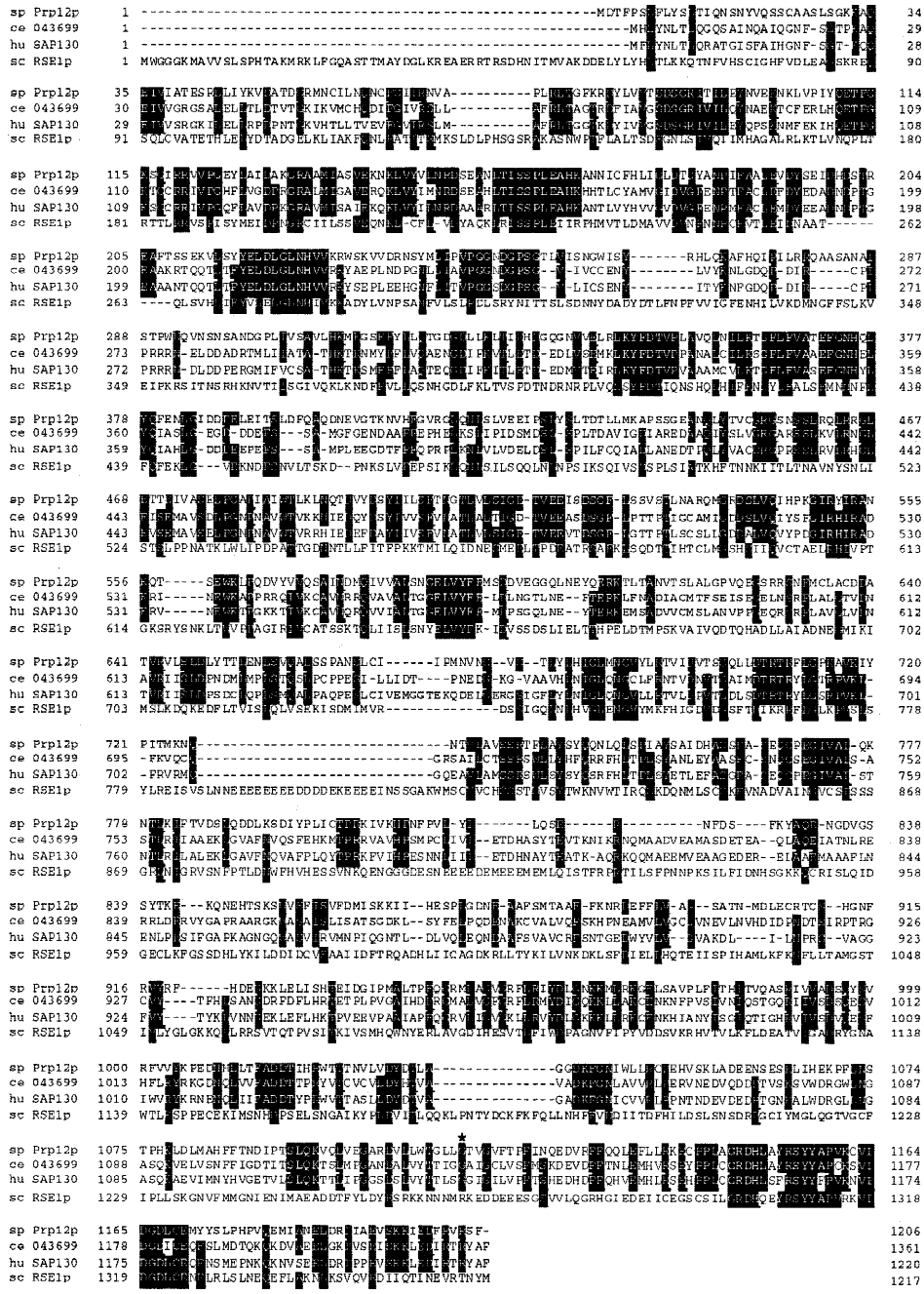

FIGURE 2. Alignment of the amino acid sequence of Prp12p with those of Prp12p homologs. Amino acids identical in all four or three proteins are highlighted by letters on a black background. The mutation site of *prp12-1* is marked with an asterisk. The alignment was carried out using the GENETYX-MAC program (Software Development Co., Ltd.). sp: *Schizosaccharomyces pombe*; sc: *Saccharomyces cerevisiae*; and ce: *Caenorhabditis elegans.*

ture, most of the *prp12-1* cells were twofold or threefold elongated compared with the wild-type cells (Fig. 5A). We also observed some abnormally elongated cells, as shown by arrowheads in Figure 5A. Most elongated *prp12-1* cells ceased growing with one nucleus at the nonpermissive temperature, except for the abnormally elongated cells, which contained two nuclei with a septum. Population of the abnormally elongated cells gradually increased along with the time of temperature shift. Fluorescence-activated cell sorter (FACS) analysis demonstrated that *prp12-1* arrested in G2 when shifted to 37 °C (Fig. 5B). On the other hand, the *cdc10-129* mutant used as a control was arrested in G1 once at 37 °C, then DNA content gradually increased due to leakiness of the mutation. After 8 h at 37 °C, cells with a 4C-DNA content accumulated in *prp12-1*. The abnormally elongated *prp12-1* cells containing two nuclei seem to be arrested with a 4C-DNA content. These results indicate

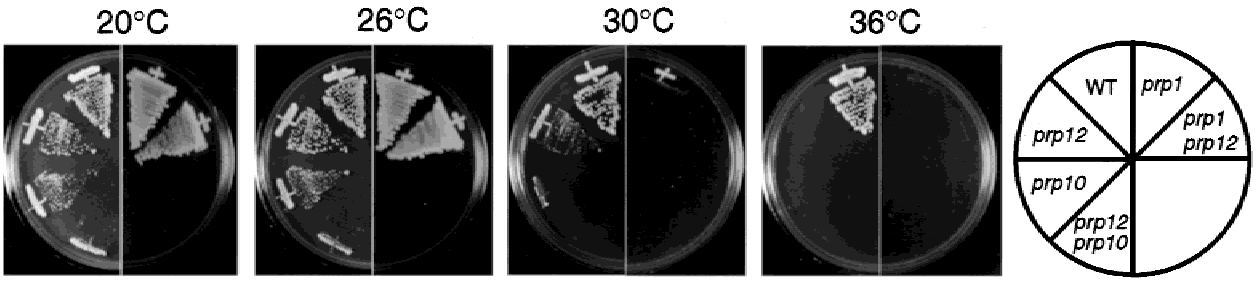

FIGURE 3. The *prp12-1 prp10-1* double mutant shows a synthetic effect on the temperature sensitivity of growth. Each strain was streaked on a YPD plate and incubated for 7 days at 20 °C, 5 days at 26 °C, or 4 days at 30 °C or 36 °C.

that *prp12-1* has a defect in G2/M transition at the nonpermissive temperature.

Kinetic analysis of the splicing defects in *prp* mutants

In addition to *prp12-1,* some other mutants (*prp5-1*, *prp8-1*, *prp11-1, prp13-1*, and *prp14-1*) produced elongated cells at the nonpermissive temperature (Urushiyama et al., 1996; Potashkin et al., 1998). On the other hand, *prp1, prp2, prp3, prp4, prp9*, and *prp10* showed no such morphological alteration even after long incubation at the nonpermissive temperature. To elucidate the reason for such a phenotypic difference between the two mutant groups, we analyzed kinetics of splicing defects in *prp1*, *prp2*, and *prp10* that do not exhibit a *cdc*-like phenotype and *prp8, prp11*, and *prp12*, which exhibit the *cdc*-like phenotype at the nonpermissive temperature. Total RNA from each strain was isolated before and after the shift to the nonpermissive temperature for 15 min, 30 min, 1 h, 2 h, 4 h, and 8 h, and subjected to northern blot analysis. For hybridization probes, we prepared ^{32}P-labeled single-stranded DNA fragments complementary to several mRNAs. Considering total intron lengths and expected expression levels, we selected *TfIId*$^+$, *rpl74*$^+$, and *ade2*$^+$ mRNAs as representative transcripts from housekeeping genes to be analyzed and *nda34*$^+$ and *cdc2*$^+$ mRNAs as representatives of the cell-cycle-related genes.

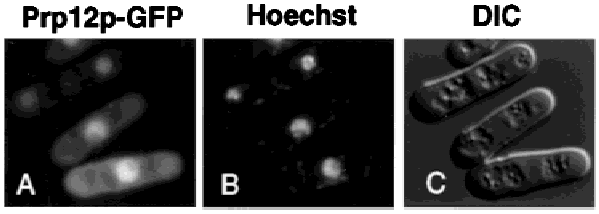

FIGURE 4. Prp12p is localized in the DNA region in the nucleus. The *prp12-1* mutant expressing GFP-tagged Prp12p was cultured to midlog phase and observed under a fluorescence microscope (**A**) after staining with Hoechst 33342 (**B**). **C** shows a differential interference contrast picture (DIC) of the corresponding field.

Results of the analyses are shown in Figure 6. Unexpectedly, we found that the splicing defect in *prp12-1* was observed only in *TfIId*$^+$ (TATA-binding protein, TBP) pre-mRNA. When using probes for transcripts from the *rpl74*$^+$, *nda34*$^+$, *cdc2*$^+$, and *ade2*$^+$ genes, we detected no splicing defects in *prp12-1*. Similar differential splicing defects were observed in *prp11-1*, which shows the *cdc*-like phenotype at the nonpermissive temperature. Splicing of the *TfIId*$^+$ and *rpl74*$^+$ pre-mRNAs is inhibited, but no significant splicing defects were detected in other mRNAs in this mutant. Interestingly, the defect in the splicing of *TfIId*$^+$ pre-mRNA seems reversible to some extent in *prp8-1* and *prp11-1*. Increasing accumulation of pre-mRNAs in these mutants was detected until 1 or 2 h after a shift in the temperature. The amounts of accumulated pre-mRNAs then decreased gradually with a concomitant reincrease of the spliced mature products (Fig. 6A). On the other hand, a rapid and almost complete inhibition of pre-mRNA splicing was observed in all analyzed genes in the mutants without the *cdc* phenotype (*prp1-4*, *prp2-1*, and *prp10-1*).

The kinetics of splicing defects was also different among genes and among alleles. Splicing of *TfIId*$^+$ pre-mRNA was more strongly and often more quickly inhibited after the shift to the nonpermissive temperature than those of four other pre-mRNAs. In addition, we tested two other *prp2* alleles (*prp2-2* and *mis11-453*; Takahashi et al., 1994) and found that the kinetics of splicing defects is slightly different among alleles (Fig. 6B). Appearance of the splicing defects in the mutant containing the *mis11-453* mutation was slower than in mutants with two other *prp2* alleles.

Splicing defects are observed in all of *TfIId*$^+$ introns in *prp12-1*

The *TfIId*$^+$ gene contains three introns with different sequences and lengths. To examine if all these introns were equally retained in the accumulated pre-mRNAs in *prp12-1* at the nonpermissive temperature, we carried out northern blot hybridization using an oligonucleotide probe complementary to each intron sequence.

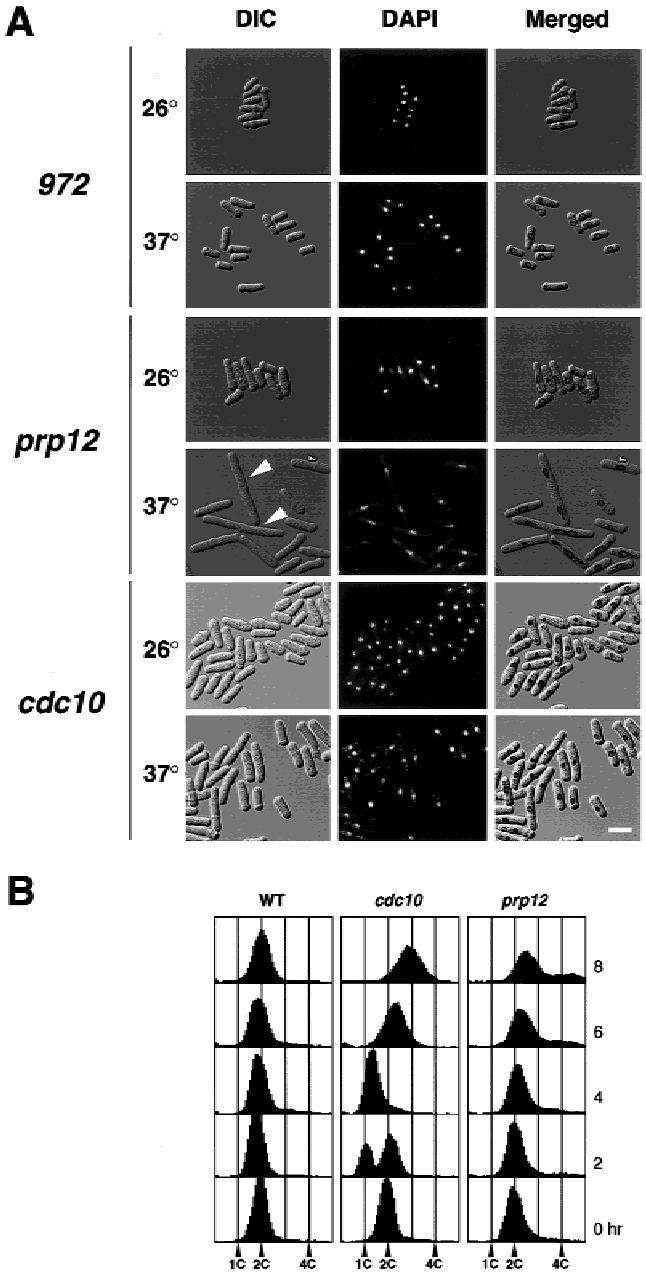

FIGURE 5. A: Cytological analysis of *prp12-1.* Wild-type (972), *cdc10-129*, and *prp12-1* were cultured at a permissive temperature of 26 °C, and then transferred to a nonpermissive temperature of 37 °C for 4 h. The cells were stained with Hoechst 33342. The first and second columns in each row show DIC pictures and pictures of cells stained with Hoechst 33342, respectively. The third column shows merged images of those pictures. Arrowheads denote the abnormally elongated cells. The bar represents 10 μm. **B:** FACS analyses. The wild-type (972), *cdc10-129*, and *prp12-1* cells cultured at 26 °C were shifted to the nonpermissive temperature for the indicated times and their DNA contents were measured with the Becton-Dickinson FACScan, as described in Materials and Methods. The DNA content and relative cell number were plotted along with x and y axes, respectively. The positions of 1C, 2C, and 4C DNA content are indicated at the bottom.

As shown in Figure 7, all the intron probes gave hybridization signals corresponding to the *TfIId*$^+$ pre-mRNA in *prp12-1.* In *prp2-2*, only RNAs from cells that were shifted to 37 °C showed hybridization signals. In *prp12-1*, hybridization signals in samples at 37 °C were stronger than those in the samples at 26 °C for all introns; however, intensities of the hybridization signals of the intron 3 probe were weaker than those of other two intron probes.

In the case of the intron 2 probe, we detected the band corresponding to the mature-size mRNA in addition to the pre-mRNA band. This band may correspond to partially spliced mRNA containing intron 2 (52 nt in length) only. These results suggest that the loss of Prp12p activity at the nonpermissive temperature in *prp12-1* affects excision of all introns in the *TfIId*$^+$ pre-mRNA, although severities of the splicing defects vary among introns.

DISCUSSION

We found that the *prp12*$^+$ gene codes for a putative homolog of human U2 snRNP associated factor, SAP130/SF3b130 (Wang et al., 1998; Das et al., 1999). As SAP130/SF3b130 is known to be a subunit of SF3b, we produced a double mutant carrying *prp12-1* and *prp10-1*, the wild-type gene of which encodes the *S. pombe* homolog of another subunit in SF3b, SAP155/SF3b155 (Habara et al., 1998). The double mutant showed synthetic lethality at 26 °C, suggesting that Prp12p interacts with Prp10p/spSAP155. This result supports the notion that Prp12p is a functional homolog of human SAP130/SF3b130.

Human SF3 is involved in binding of U2 snRNP to the branch site in the splicing reaction. The interaction between each of the SF3 subunits and the pre-mRNA sequences around the branch point sequence was analyzed by the UV-crosslink assay (Gozani et al., 1996). SF3 subunits except for SAP130/SF3b130 crosslinked with the nucleotides at the 5′-side of the branch site called an anchoring site. SAP130/SF3b130 did not bind to pre-mRNA directly (Gozani et al., 1996). Therefore, it is possible that SAP130/Prp12p has a role different from those of other SF3 subunits, although the exact function of each SAP in pre-mRNA splicing is still unknown.

An interesting phenotype of *prp12-1* is a substrate-specific splicing defect at the nonpermissive temperature. In the analyzed pre-mRNAs, only *TfIId*$^+$ pre-mRNA showed splicing defects at the nonpermissive temperature. As we detected a small amount of unspliced *TfIId*$^+$ pre-mRNA even in the wild-type cells (Fig. 6A), *TfIId*$^+$ pre-mRNA appears to be a substrate with low splicing efficiency in vivo. Thus, one explanation for the substrate-specific splicing defect in *prp12-1* is that mutated Prp12p produced from the *prp12-1* allele retains residual activity even at the nonpermissive temperature, which does not affect splicing of efficiently spliced transcripts but does cause splicing inhibition in “poor” splicing substrates, such as *TfIId*$^+$

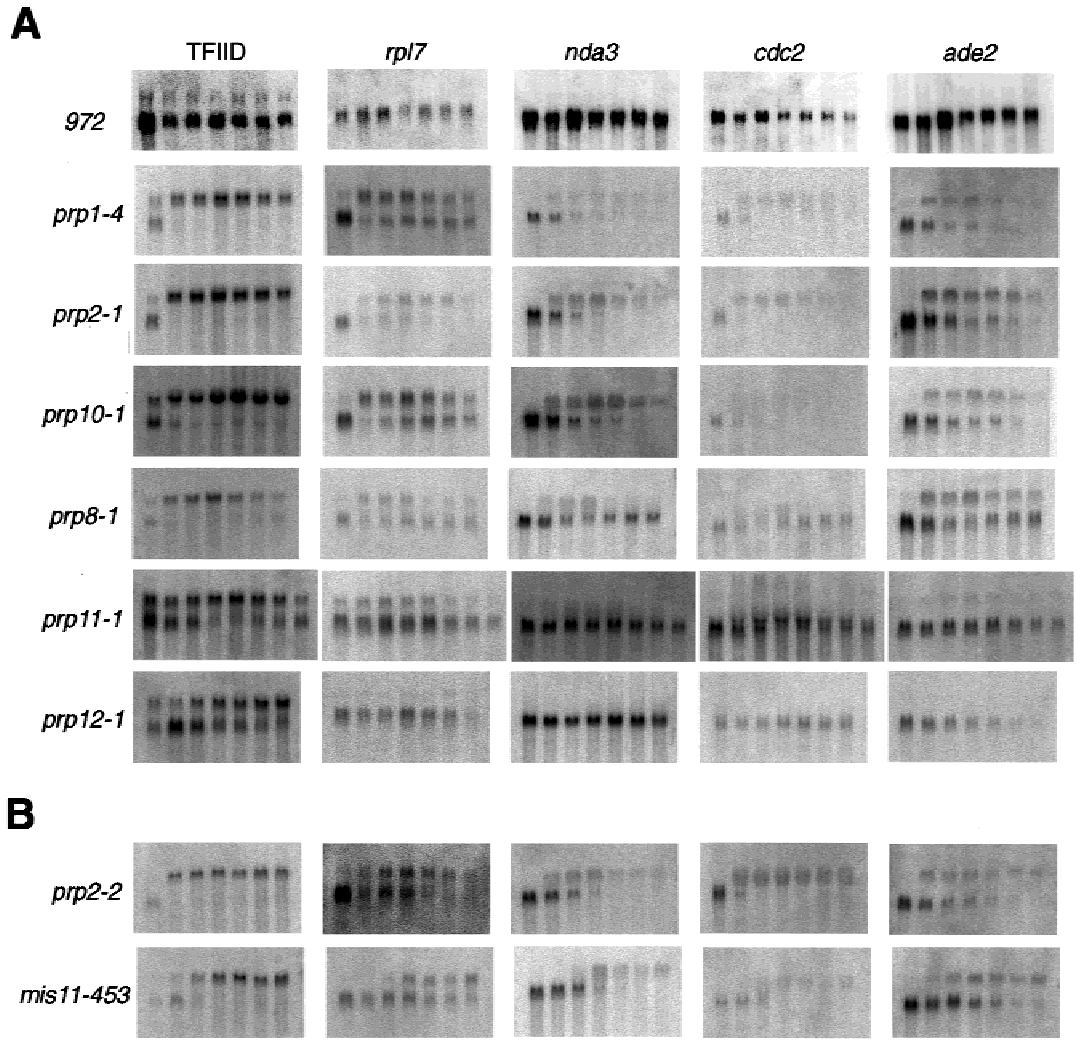

FIGURE 6. A: Kinetic analysis of the splicing defects in *prp12-1* and some *prp* mutants at the nonpermissive temperature. Each mutant, except for *prp11-1*, was grown in a YPD medium at 26 °C, and midlog cultures were shifted to 37 °C. In the case of the *cs* mutant *prp11-1*, culturing was done at 32 °C and then the mid-log culture was shifted down to 22 °C. Total RNAs were prepared before shifting and after the temperature shift for 15 min, 30 min, 1 h, 2 h, 4 h, and 8 h, and subjected to northern blot hybridization with the indicated ^{32}P-labeled probe. Membranes were exposed to a Fuji imaging plate and analyzed using a Bioimaging Analyzer BAS-1000 (Fuji Photo Film Co., Ltd.). Each panel shows the results on RNAs before shifting and 15 min, 30 min, 1, 2, 4, or 8 h (and 16 h in the case of *prp11-1*) after the shift from left to right. **B:** Kinetics of splicing defects differed among alleles. The *prp2* mutants with two distinct alleles (*prp2-2* and *mis11-453*) were subjected to northern blot analysis as described in **A**.

pre-mRNA. The fact that the *prp12-1* gene in the multicopy vector suppressed the temperature sensitive phenotype of the mutation supports the notion that *prp12-1* is not a null mutation.

The *S. cerevisiae* homolog of Prp12p was found to be Rse1p (Chen et al., 1998). *rse1* was originally isolated as a mutant defective in ER-to-Golgi transport in *S. cerevisiae*. Chen et al. (1998) reported that the phenotype of ER-to-Golgi transport defects in *rse1-1* is caused by a splicing defect in the *SAR1* gene, which contains a single short intron and encodes a small GTP-binding protein required for COPII vesicle formation from the endoplasmic reticulum. They also found that expression of the artificial intronless *SAR1* gene in *rse1-1* partially suppresses its temperature sensitivity (Chen et al., 1998). This finding suggests that splicing of the *SAR1* pre-mRNA is more strongly affected by the *rse1-1* mutation than splicing of other pre-mRNAs. In *S. pombe*, Romfo et al. (1999) reported differential sensitivity of introns in pre-mRNA splicing to mutational inactivation of the *prp2*$^{+}$ gene, which encodes a large subunit of the U2AF heterodimer (U2AF^{59}). Differential sensitivity of pre-mRNAs to a *prp* mutation in splicing may account for the substrate-specific splicing defect observed in *prp12-1*.

An alternative explanation for the substrate-specific splicing defects in *prp12-1* is a requirement of Prp12p for splicing of some specific pre-mRNAs. However, this

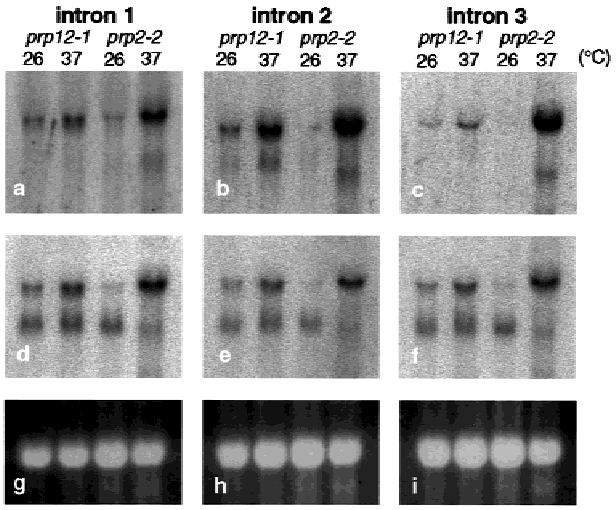

FIGURE 7. Comparison of defect in excision of each intron in the *TfIId*$^+$ pre-mRNA. *prp2-2* and *prp12-1* were cultured at 26 °C to the midlog phase and either maintained at 26 °C or shifted to 37 °C for 2 h. Total RNAs were then isolated and subjected to northern blot hybridization using each TFIID intron probe as indicated (**a**–**c**). After analysis using BAS-1000, membranes were reprobed with the TFIID exon probe to determine the quantities of *TfIId*$^+$ pre-mRNA and mature mRNA on each filter (**d**–**f**). Panels **g** to **i** indicate the 28S rRNA stained with ethidium bromide, which indicate the quantity of total RNA present in each lane.

seems unlikely, because mutation of Prp10p in the same SF3b complex showed no such substrate-specific splicing inhibition (Habara et al., 1998).

The low splicing efficiency in *TfIId*$^+$ pre-mRNA seems to be independent of the number and size of introns within the gene. The number of introns, their sizes, and sequences of the splice sites in each analyzed genes are shown in Table 1. It is notable that *TfIId*$^+$ pre-mRNA contains purine-rich sequences between the presumed branch sites and 3′ splice sites in introns 1 and 2. The presence of such a purine-rich sequence in this region might explain the "poor" splicing efficiency of *TfIId*$^+$ pre-mRNA. In mammalian splicing system, the polypyrimidine tract located between the branchpoint and 3′ splice site is required for binding of U2AF^{65} and lack of this tract drastically reduces splicing efficiency in vitro (Coolidge et al., 1997), although polypyrimidine tracts are relevant to, but not the sole determinant of, U2AF^{59} requirements for splicing in *S. pombe* (Romfo & Wise, 1997; Romfo et al., 1999).

Another interesting phenotype of *prp12-1* is elongation of the cell bodies (the *cdc* phenotype) at the nonpermissive temperature. It has been known that some *prp* mutants show a similar *cdc* phenotype at the nonpermissive temperature (Urushiyama et al., 1996; Potashkin et al., 1998). Using northern blot analysis, we found a clear difference in the kinetics of splicing inhibition between *prp* mutants without the *cdc* phenotype (*prp1*, *prp2*, and *prp10*) and those exhibiting the *cdc* phenotype (*prp8*, *prp11*, and *prp12*). The former mutant group showed splicing inhibition for all tested pre-mRNAs, and their inhibition after a shift to the nonpermissive temperature was rapid and almost complete. In contrast, in *prp12-1*, the analyzed pre-mRNAs except for *TfIId*$^+$ pre-mRNA were spliced normally even 8 h after a shift to the nonpermissive temperature, as described above. *prp8-1* and *prp11-1* also showed similar differential splicing defects among tested pre-mRNAs.

TABLE 1. Sequences of exon–intron boundaries and putative branch sites in the genes used for northern blot analysis.

Gene	ORF length		Intron length	5′ ss	Branch	3′ ss
TFIID	696	1	255	AGA GTAAGT	TACTAAT	AATCCTCTTAAAA TAG CTG
		2	52	AAA GTACGT	TATTGAC	CAAACA TAG CGT
		3	70	TCT GTAAGT	ATCTAAC	TGTTCTTTTT TAG TAT
rpl7	753	1	290	GAG GTATGT	TACTAAT	TTTACTC CAG GCC
nda3	1341	1	36	ATT GTACGA	AGCTAAT	CAA TAG GTT
		2	52	TTG GTAAGC	AACTAAC	GCTTGG AAG GTC
		3	41	AAT GTAGGT	TACTGAC	TTTTACG TAG ATA
		4	89	GAG GTAGGT	TACTGAC	GACTG TAG GCC
		5	85	ATG GTATGT	TGCTAAC	CTCGAAA TAG TCC
ade2	1302	1	39	TGG GTAAGA	AATTTAC	TATTCACA CAG AAT
		2	383	CAG GTATGT	AGCTAAC	TTTTATTTT TAG GGT
cdc2	894	1	68	AAG GTAGGT	TACTGAC	TAATGC TAG GAA
		2	71	TCG GTAAGT	TTCTAAC	CCTTTTTT AAG ACT
		3	101	GAG GTATAT	CGCTAAC	CGTT TAG ATT
		4	54	TCT GTAAGA	TACTAAC	CATTTTGTC AAG GCT
consensus				GTANGT	CTRAY	NAG

Sequences used in this table were taken from the EMBL/GenBank/DDBJ database with accession no. X53415 for TFIID, X53575 for *rpl7*, M10347 for *nda3*, M98805 for *ade2,* and M12912 for *cdc2*. The branch site in each intron was presumed by comparing with the consensus branch sequence and based on the distance from the 3′ splice site. The consensus sequence was derived from Prabhala et al. (1992). Y: pyrimidine, R: purine.

In *S. pombe*, over 45% of the genes have introns. Therefore, complete inhibition of pre-mRNA splicing in the mutants will result in immediate block of cell metabolism and cell growth. If this is the case, then cells with a tight *prp* mutation, such as *prp2*, may stop growing at various stages of the cell cycle. On the other hand, in cells with a weak *prp* mutation such as *prp12-1*, only transcripts sensitive to the mutation will show splicing defects, which cause a disturbance of specific intracellular reactions in which products from the transcripts are involved.

Most *prp12-1* cells shifted to the nonpermissive temperature showed elongated cell bodies with a single nucleus (Fig. 5; Urushiyama et al., 1996). In addition, FACS analyses revealed that most of those arrested cells contain a 2C DNA content. Thus, *prp12-1* is likely to have a defect in G2/M transition at the nonpermissive temperature. If *S. pombe* has an intron-containing gene involved in G2/M transition and splicing of its transcripts is sensitive to the *prp12* mutation, then the G2/M transition in *prp12-1* would be perturbed at the nonpermissive temperature, leading to elongation of the cell bodies, that is, the *cdc* phenotype.

Splicing of *cdc2*$^+$ pre-mRNA involved in G2/M transition was not inhibited by the *prp12* mutation (Fig. 6). Thus far, we have not found a rate-limiting gene to explain the *cdc*-like phenotype observed in the *prp12-1* mutant. Besides *cdc2*, there are intron-containing genes involved in G2/M transition or S phase progression in *S. pombe*. Analyses of transcripts from those genes are now in progress to identify a rate-limiting gene(s) leading to the *cdc* phenotype.

On the other hand, there are reports indicating the direct relation between splicing reaction and cell-cycle control, such as phosphorylation of SAP155/SF3b155 by cyclin E-cdk2 (Seghezzi et al., 1998). Also, we cannot explain why *zer1*, an allele of *prp1,* is arrested at G0 when shifted to the nonpermissive temperature based on the scenario described above. If the scenario is applicable for all *prp* mutations, then all weak *prp* mutants should be arrested at the same rate-limiting step, that is, G2/M. To elucidate exact mechanisms of the relationship between pre-mRNA splicing and cell-cycle control, it is necessary to analyze cell-cycle defects in mutants with alleles showing a strong splicing inhibition and those with a weak splicing defect in the same *prp* gene.

We found that defects in the pre-mRNA splicing in *prp8-1* and *prp11-1* were eliminated to some extent after 1 or 2 h shifting to the nonpermissive temperature, indicating that there is a mechanism compensating the functions of Prp8p and Prp11p, which are a DEAH box RNA helicase (Lundgren et al., 1996) and a DEAD box RNA helicase (S. Urushiyama, K. Saeki, Y. Ohshima, & T. Tani, unpubl. results), respectively, when their activities are lost. To our knowledge, this is a first observation of reversible splicing defects in *prp* mutants. Mechanisms linked to such "adaptation" in pre-mRNA splicing are subjects of ongoing studies.

MATERIALS AND METHODS

Yeast strains and general methods

S. pombe strains used in this study are listed in Table 2. Standard genetical procedures for *S. pombe* were as described (Moreno et al., 1991; Alfa et al., 1993). Transformation of *S. pombe* with a cosmid library was done as described (Okazaki et al., 1990). Isolation of haploids with double mutations was carried out as described previously (Urushiyama et al., 1997).

Preparation of RNA and northern blot analysis

Preparation of total RNA for northern blot analysis was carried out as described (Urushiyama et al., 1996). For kinetic analysis of the splicing defect, we labeled the DNAs using a Taq DNA polymerase. We cloned partial fragments of several genes and used them as templates for the polymerase reaction. The cloned genes are *TfIId*$^+$ (TATA binding protein; X53415; Hoffmann et al., 1990), *nda34*$^+$ (β-tubulin; M10347; Hiraoka et al., 1984), *cdc2*$^+$ (cyclin dependent kinase; M12912; Hindley & Phear, 1984), *rpl74*$^+$ (ribosomal protein L7; X53575; Murray & Watts, 1990), and *ade2*$^+$ (adenylsuccinate synthetase; M98805; Speiser et al., 1992). Isolations of the partial gene fragments were done by PCR using primers with a restriction site at their 5′ ends. The amplified products were cloned in Bluescript vector (Stratagene). The resultant plasmids were then cut with a restriction enzyme (*Eco*RI for *TfIId*$^+$, *rpl74*$^+$, *cdc2*$^+$, and *ade2*$^+$, and *Eco*T22I for *nda34*$^+$) to be linearized. To obtain a single-stranded ^{32}P-labeled DNA probe, the polymerase reaction was carried out with a single primer and the Taq DNA polymerase using

TABLE 2. List of *S. pombe* strains used in this study.

Strain	Genotype	Source
972	*h*$^-$	Gutz et al., 1974
SU26-9B	*h*$^-$, *prp8-1*	Urushiyama et al., 1996
SU35-3A	*h*$^+$, *prp2-1*	Urushiyama et al., 1996
SU50-4D	*h*$^+$, *prp2-2*	Urushiyama et al., 1996
SU59-1D	*h*$^-$, *leu1-32*	Urushiyama et al., 1996
SU93-2D	*h*$^-$, *prp11-1*	Urushiyama et al., 1996
SU100-2A	*h*$^-$, *prp12-1*	Urushiyama et al., 1996
SU102-11D	*h*$^-$, *prp12-1, leu1-32*	Urushiyama et al., 1996
SU149-19B	*h*$^-$, *prp1-4, prp12-1*	Urushiyama et al., 1996
MIS11	*h*$^-$, *mis11-453, leu1-32*	Takahashi et al., 1994
HB3-1C	*h*$^-$, *mis11-453*	This study
HB7-3A	*h*$^-$, *prp12-1, prp10-1*	This study
YH12	*h*$^-$, *ura4-D18, int[prp12*$^+$, *ura4*$^+$*]*	This study
YH15	*h*$^+$, *prp12-1, ura4-D18*	This study
UR105	*h*$^-$, *prp1-4*	Urushiyama et al., 1996
UR230	*h*$^-$, *prp10-1*	Urushiyama et al., 1996
UR441	*h*$^-$, ura4-D18	Urushiyama et al., 1996
CDC10	*h*$^-$, *cdc10-129*	P. Nurse

the linearized plasmid as a template in the presence of ^{32}P-dCTP. After the reaction, the products were purified using Probe Quant G-50 microcolumns (Pharmacia).

Northern blot analysis using an oligonucleotide probe for each *TfIId*$^+$ intron was done as described (Urushiyama et al., 1996). The sequences of the oligonucleotides used for amplification of the gene fragments (the first two sequences in each set) and for labeling the probes (the last one) are as follows:

TFIID

5′-CGG AAT TCC GCT GTT ATT ATG CGT ATC-3′;
5′-CGG GAT CCG TGA TAA CTG TTG ACA TGC C-3′;
5′-AAA GTA CCG TGG GAG TAA GC-3′.

rpl7

5′-GCG AAT TCC CAG AAG AAA AAT CGT AAA G-3′;
5′-CGG GAT CCT TAA ATT CCA ATC CAC GGC C-3′;
5′-TCA TAT TTG CCC AAG GCC TC-3′.

nda3

5′-CAT GGT TTG GAT TCA GCT GG-3′;
5′-TAT CGG GAA TCC ACT CAA CG-3′;
5′-GAA CAG AGC GAA TTT GCT CG-3′.

cdc2

5′-CGG AAT TCT TTT GGA TAT TTT ACA TGC TG-3′;
5′-CGG GAT CCT TTG CAC TAA TGC GAT GGG C-3′;
5′-CTC ATG CGT ATA GTT CCG CA-3′.

ade2

5′-CGG AAT TCA CAT TCT TCC TTC AGG AC-3′;
5′-CGG GAT CCA ACA CCG ATG AAA GTG ATG-3′;
5′-TCT GCA AGT CAG CAA CGT TC-3′.

TFIID intron 1 probe

5′-CGT ATC ATC CCC TGC GGT CAT TGC CTT CGG-3′.

TFIID intron 2 probe

5′-GAC CTC AAA CAA AAT TAA AAG GGT TTA ACG-3′.

TFIID intron 3 probe

5′-CAG CAA CAA CAT CTT TAA AGA TGA TGA ACT-3′.

Localization of GFP-tagged Prp12p

For expression of GFP-tagged Prp12p, the *prp12*$^+$ gene containing the *Nde*I genomic fragment was cloned into pSP1. On the other hand, the 3′-end fragment of the *prp12*$^+$ gene was prepared by PCR using the primers pp12-40 (5′-TCACCAA TCGCTTATTCTGC-3′) and pp12-link-1 (5′-CGCGGATCC TCTAGACGTCTGCAGAAAACTACGAACACGAAAATC-3′). Then, the region from the *Nhe*I site to the 3′ end was replaced with the PCR fragment digested with *Nhe*I and *Bam*HI. The resultant plasmid has the insert containing the *prp12*$^+$ promoter and full-length ORF except for a stop codon followed by the linker sequence with restriction sites. The fragment containing the GFP gene was prepared from pEGFP-N1 (Clontech), which was digested with *Xba*I and *Pst*I. The GFP fragment was then inserted into the *Xba*I and *Pst*I sites of the *prp12*$^+$ gene containing plasmid described above. After sequencing to confirm in-frame ligation, we introduced the plasmid into the SU102-11D or SU59-1D strain. Temperature sensitivity of *prp12-1* for growth was complemented by this construct, suggesting that the fusion gene is functional in *S. pombe*. After culturing at 26 °C, the SU59-1D transformant was permeabilized using ethanol, stained with 0.5 μg/mL Hoechst 33342 (Sigma) for 5 min and observed under an Olympus AX70 fluorescence microscope equipped with a Photometrics Quantix cooled CCD camera to examine localization of Prp12p tagged with GFP.

Integration mapping

To determine if the complementing fragment (*Nde*I 5.7 kb) contained the *prp12*$^+$ gene, chromosomal integration mapping was performed. The *Nde*I 5.7-kb genomic fragment (Fig. 1) was subcloned into a pBluescript-ura4 vector containing the *ura4*$^+$ gene in the Bluescript vector. Then the resultant plasmid was linearized by a restriction enzyme *Bgl*II and introduced into UR441. Stable Ura4$^+$ transformants were isolated and integration of the *ura4*$^+$ gene in the gene locus between cosmids c27E2 and c19G12 was confirmed by PCR. The obtained strain (YH12) was crossed with YH15 and asci were dissected on YPDA plates. We analyzed 23 asci, and spores from all of them showed parental ditype.

Fluorescence-activated cell sorting (FACS) analysis

FACS analysis was carried out essentially as described previously (Alfa et al., 1993). A total of 2×10^6 exponentially growing cells cultured at 26 °C or shifted to 37 °C for indicated time were suspended in 70% ethanol and kept at 4 °C overnight. After washing with 1 mL of 50 mM sodium citrate, the fixed cells were resuspended in 1 mL of a solution containing 50 mM sodium citrate, 0.1 mg/mL RNase A, and 2 μg/mL propidium iodide and were subjected to analysis using a Becton-Dickinson (San Jose, California) FACScan.

ACKNOWLEDGMENTS

We thank Drs. Judith Potashkin and David Frendewey for providing the *prp* mutants, Dr. Mitsuhiro Yanagida for providing the *mis11* strain, and Dr. Robin Reed and coworkers for sharing the sequence of SAP130/SF3b130 with us prior to publication. We also thank Eri Hirosawa and Sin Hwang for their technical assistance. Language assistance was provided by M. Ohara. This work was supported by grants from the Ministry of Education, Science, Sports and Culture of

Japan to T.T. and Y.O. and by a grant from the Japan Science and Technology Corporation to T.T.

Received July 6, 2000; returned for revision July 25, 2000; revised manuscript received February 7, 2001

REFERENCES

Alahari SK, Schmidt H, Käufer NF. 1993. The fission yeast *prp4*$^+$ gene involved in pre-mRNA splicing codes for a predicted serine/threonine kinase and is essential for growth. *Nucleic Acids Res 21*:4079–4083.

Alfa C, Fantes P, Hyams J, McLeod M, Warbrick E. 1993. Experiments with fission yeast. A laboratory course manual. Cold Spring Harbor, New York: Cold Spring Harbor Laboratory Press.

Aves SJ, Durkacz BW, Carr A, Nurse P. 1985. Cloning, sequencing and transcriptional control of the *Schizosaccharomyces pombe cdc10* 'start' gene. *EMBO J 4*:457–463.

Bennett M, Reed R. 1993. Correspondence between a mammalian spliceosome component and an essential yeast splicing factor. *Science 262*:105–108.

Burge CB, Tuschl T, Sharp PA. 1999. Splicing of precursors to mRNAs by the spliceosomes. In: Gesteland RF, Cech TR, Atkins JF, eds. *The RNA world*. Cold Spring Harbor, New York: Cold Spring Harbor Laboratory Press. pp 525–560.

Chen EJ, Frand AR, Chitouras E, Kaiser CA. 1998. A link between secretion and pre-mRNA processing defects in *Saccharomyces cerevisiae* and the identification of a novel splicing gene, *RSE1*. *Mol Cell Biol 18*:7139–7146.

Coolidge CJ, Seely RJ, Patton JG. 1997. Functional analysis of the polypyrimidine tract in pre-mRNA splicing. *Nucleic Acids Res 25*:888–896.

Cottarel G, Beach D, Deuschle U. 1993. Two new multi-purpose multicopy *Schizosaccharomyces pombe* shuttle vectors, pSP1 and pSP2. *Curr Genet 23*:547–548.

Das BK, Xia L, Palandjian L, Gozani O, Chyung Y, Reed R. 1999. Characterization of a protein complex containing spliceosomal proteins SAPs 49, 130, 145, and 155. *Mol Cell Biol 19*:6796–6802.

Gozani O, Feld R, Reed R. 1996. Evidence that sequence-independent binding of highly conserved U2 snRNP proteins upstream of the branch site is required for assembly of spliceosomal complex A. *Genes & Dev 10*:233–243.

Gozani O, Potashkin J, Reed R. 1998. A potential role for U2AF-SAP155 interactions in recruiting U2 snRNP to the branch site. *Mol Cell Biol 18*:4752–4760.

Groß T, Lützelberger M, Wiegmann H, Klingenhoff A, Shenoy S, Käufer NF. 1997. Functional analysis of the fission yeast Prp4 protein kinase involved in pre-mRNA splicing and isolation of a putative mammalian homologue. *Nucleic Acids Res 25*:1028–1035.

Gutz H, Helslot H, Leupold U, Loprieno N. 1974. *Schizosaccharomyces pombe*. In: King RC, ed. *Handbook of genetics*. New York: Plenum Press. pp 395–446.

Habara Y, Urushiyama S, Tani T, Ohshima Y. 1998. The fission yeast *prp10*$^+$ gene involved in pre-mRNA splicing encodes a homologue of highly conserved splicing factor, SAP155. *Nucleic Acids Res 26*:5662–5669.

Hindley J, Phear GA. 1984. Sequence of the cell division gene *CDC2* from *Schizosaccharomyces pombe*; patterns of splicing and homology to protein kinases. *Gene 31*:129–134.

Hiraoka Y, Toda T, Yanagida M. 1984. The NDA3 gene of fission yeast encodes beta-tubulin: A cold-sensitive *nda3* mutation reversibly blocks spindle formation and chromosome movement in mitosis. *Cell 39*:349–358.

Hoffmann A, Horikoshi M, Wang CK, Schroeder S, Weil PA, Roeder RG. 1990. Cloning of the *Schizosaccharomyces pombe* TFIID gene reveals a strong conservation of functional domains present in *Saccharomyces cerevisiae* TFIID. *Genes & Dev 4*:1141–1148.

Krämer A. 1995. In: Lamond AI ed. *Pre-mRNA processing*. Heidelberg, Germany: Springer-Verlag, pp 35–64.

Krämer A. 1996. The structure and function of proteins involved in mammalian pre-mRNA splicing. *Annu Rev Biochem 65*:367–409.

Krämer A, Legrain P, Mulhauser F, Gröning K, Brosi R, Bilbe G. 1994. Splicing factor SF3a60 is the mammalian homologue of PRP9 of *S. cerevisiae*: The conserved zinc finger-like motif is functionally exchangeable in vivo. *Nucleic Acids Res 22*:5223–5228.

Lundgren K, Allan S, Urushiyama S, Tani T, Ohshima Y, Frendewey D, Beach D. 1996. A connection between pre-mRNA splicing and the cell cycle in fission yeast: *cdc28*$^+$ is allelic with *prp8*$^+$ and encodes an RNA-dependent ATPase/helicase. *Mol Biol Cell 7*:1083–1094.

McDonald WH, Ohi R, Smelkova N, Frendewey D, Gould KL. 1999. Myb-related fission yeast cdc5p is a component of a 40S snRNP-containing complex and is essential for pre-mRNA splicing. *Mol Cell Biol 19*:5352–5362.

Moreno S, Klar A, Nurse P. 1991. Molecular genetic analysis of fission yeast *Schizosaccharomyces pombe*. *Methods Enzymol 194*:795–823.

Murray JM, Watts FZ. 1990. Isolation of a *Schizosaccharomyces pombe* homologue to the rat ribosomal protein, L7. *Nucleic Acids Res 18*:4590.

Nakaseko Y, Adachi Y, Funahashi S, Niwa O, Yanagida Y. 1986. Chromosome walking shows a highly homologous repetitive sequence present in all the centromere regions of fission yeast. *EMBO J 5*:1011–1021.

Okazaki K, Okazaki N, Kume K, Jinno S, Tanaka K, Okayama H. 1990. High frequency transformation method and library transducing vectors for cloning mammalian cDNAs by trans-complementation of *Schizosaccharomyces pombe*. *Nucleic Acid Res 18*:6485–6489.

Potashkin J, Frendewey D. 1989. Splicing of the U6 RNA precursor is impaired in fission yeast pre-mRNA splicing mutant. *Nucleic Acids Res 17*:7821–7831.

Potashkin J, Kim D, Fons M, Humphrey T, Frendewey D. 1998. Cell-division-cycle defects associated with fission yeast pre-mRNA splicing mutants. *Curr Genet 16*:153–163.

Potashkin J, Naik K, Wentz-Hunter K. 1993. U2AF homologue required for splicing in vivo. *Science 262*:573–575.

Prabhala G, Rosenberg GH, Käufer NF. 1992. Architectural features of pre-mRNA introns in the fission yeast *Schizosaccharomyces pombe*. *Yeast 8*:171–182.

Romfo CM, Lakhe-Reddy S, Wise JA. 1999. Molecular genetic analysis of U2AF^{59} in *Schizosaccharomyces pombe*: Differential sensitivity of introns to mutational inactivation. *RNA 5*:49–65.

Romfo CM, Wise JA. 1997. Both the polypyrimidine tract and the 3′ splice site function prior to the first step of splicing in fission yeast. *Nucleic Acids Res 25*:4658–4665.

Rosenberg GH, Alahari SK, Käufer NF. 1991. *prp4* from *Schizosaccharomyces pombe*, a mutant deficient in pre-mRNA splicing isolated using genes containing artificial introns. *Mol Gen Genet 226*:305–309.

Seghezzi W, Chua K, Shanahan F, Gozani O, Reed R, Lees E. 1998. Cyclin E associates with components of the pre-mRNA splicing machinery in mammalian cells. *Mol Cell Biol 18*:4526–4536.

Speiser DM, Ortiz DF, Kreppel L, Scheel G, McDonald G, Ow DW. 1992. Purine biosynthetic genes are required for cadmium tolerance in *Schizosaccharomyces pombe*. *Mol Cell Biol 12*:5301–5310.

Takahashi K, Yamada H, Yanagida M. 1994. Fission yeast minichromosome loss mutants *mis* cause lethal aneuploidy and replication abnormality. *Mol Biol Cell 5*:1145–1158.

Urushiyama S, Tani T, Ohshima Y. 1996. Isolation of novel pre-mRNA splicing mutants of *Schizosaccharomyces pombe*. *Mol Gen Genet 253*:118–127.

Urushiyama S, Tani T, Ohshima Y. 1997. The *prp1*$^+$ gene required for pre-mRNA splicing in *Schizosaccharomyces pombe* encodes a protein that contains TPR motifs and is similar to Prp6p of budding yeast. *Genetics 147*:101–115.

Wang C, Chua K, Seghezzi W, Lees E, Gozani O, Reed R. 1998. Phosphorylation of spliceosomal protein SAP155 coupled with splicing catalysis. *Genes & Dev 12*:1409–1414.

Wentz-Hunter K, Potashkin J. 1996. The small subunit of the splicing factor U2AF is conserved in fission yeast. *Nucleic Acids Res 24*:1849–1854.